

SUPPORTING INFORMATION

A general method for cultivating single crystals from melt microdroplets

Xiao Ou,^{a,†} Xizhen Li,^{a,†} Haowei Rong,^a Lian Yu,^c Ming Lu^{*a,b}

^a School of Pharmaceutical Sciences, Sun Yat-sen University, Guangzhou, China

^b Guangdong Provincial Key Laboratory of New Drug Design and Evaluation, Sun Yat-sen University, Guangzhou, China

^c School of Pharmacy, University of Wisconsin – Madison, Madison, Wisconsin, USA

Electronic Supporting Information

Table of Contents

1. Materials	S3
2. Experimental details.....	S3
2.1 Single-crystal X-ray diffraction.	S3
2.2 Powder X-ray diffraction (PXRD).	S3
2.3 Differential scanning calorimetry (DSC)	S3
3. Results	S4
3.1 General principle of cultivating single crystals from melt microdroplets.....	S4
3.2 Griseofulvin polymorphs	S4
3.3 Cultivation of single crystals of twenty clinical drugs using melt microdroplet method.....	S6
(1) Crizotinib	S6
(2) Lorlatinib	S7
(3) Gefitinib	S8
(4) Axitinib	S9
(5) Griseofulvin (Form I)	S10
(6) Fluconazole	S11
(7) Clotrimazole	S12
(8) Ciclopirox	S13
(9) Nifedipine.....	S14
(10) Felodipine.....	S15
(11) Nimodipine.....	S16
(12) Nitrendipine	S17
(13) Gliclazide	S18
(14) Repaglinide	S19
(15) Metformin hydrochloride	S20
(16) Vildagliptin	S21
(17) Paracetamol	S22
(18) Aspirin	S23
(19) Celecoxib	S24
(20) Indomethacin	S25

1. Materials

Griseofulvin, fluconazole, clotrimazole, ciclopirox, nifedipine, felodipine, nimodipine, nitrendipine, gliclazide, metformin hydrochloride, vildagliptin, paracetamol, aspirin, celecoxib and indomethacin were purchased from Aladdin Reagent Int. (Shanghai, China). Crizotinib, lorlatinib, gefitinib, axitinib and repaglinide were purchased from ChemShuttle (Wuxi, China).

2. Experimental details

2.1 Single-crystal X-ray diffraction

Single crystals were synthesized by the present method using Linkam hot stage (THM S600, Waterfield, UK) combined with a Nikon microscopy (Nikon eclipse lv100N pol). Single-crystal X-ray diffraction data were collected on an XtaLAB Synergy with Cu K α radiation ($\lambda = 1.54184 \text{ \AA}$). Cell refinement and data reduction were carried out by CrysAlisPro 171.40 (Rigaku). The crystal structure was solved by intrinsic phasing methods using SHELXT (Sheldrick, 2015) and refined by full-matrix least-squares using SHELXL (Sheldrick, 2015) in Olex 2-1.3 (Dolomanov et al., 2009). The simulated PXRD pattern was calculated using Mercury 4.2.0.

2.2 Powder X-ray diffraction (PXRD)

PXRD patterns were recorded using a Rigaku D-MAX/2200 VPC X-ray diffractometer, using Cu K α radiation with $\lambda = 1.54056 \text{ \AA}$ in 40 kV and 26 mA condition. The samples were placed on a monocrystalline silicon plate and scanned from 5° to 45° (2θ) with a scanning speed of $2\text{-}6^\circ/\text{min}$.

2.3 Differential scanning calorimetry (DSC)

DSC thermograms were recorded using a Netzsch DSC 200-F3 (Netzsch group, Germany).

3. Results

3.1 General principle of cultivating single crystals from melt microdroplets

The general principle of cultivating single crystals from melt microdroplets is to obtain the parent polycrystals first and then partially melt only a small quantity of the sample to make a single-crystal seed in an isolated melt microdroplet. This seed is grown near its melting point into a single crystal with sufficient size and quality for X-ray diffraction. The polycrystalline material used for this procedure can be obtained by spontaneous nucleation, which is the case for GSF Form III, or other means.

3.2 Griseofulvin polymorphs

Preparation of pure polycrystalline GSF Form III sample. To grow polycrystalline sample of GSF Form III, commercial GSF powder was melted at 495 K between two coverslips and then quenching to room temperature, followed by isothermally crystallizing at 383 K for 48 h to trigger the nucleation of GSF Form III. The use of crystallization between two coverslips and a very low nucleation temperature (only 21 K above the glass transition temperature of GSF, 362 K^[1]) effectively depressed the nucleation of fast-growing Form I, but the cost is an extralong nucleation induction period for Form III. The addition of 10%wt polyethylene glycols can shorten the nucleation induction time of Form III to less than 30 min, but this will enhance the nucleation probability of Form I. Once small spherulites of GSF Form III appeared, Form III seeds were introduced to a melt droplet at 453 K using a stainless-steel needle and grown to consume the remaining melt within tens of minutes. This can yield pure polycrystals of Form III.

Preparation of pure polycrystalline GSF Form II sample. A Form III sample was held at 478 K for 1 min to trigger the solid-solid polymorphic conversion, and then was heated at 483 K for melting all Form III crystals, followed by isothermally crystallizing at 473 K for 15 min to yield pure Form II.

SUPPORTING INFORMATION

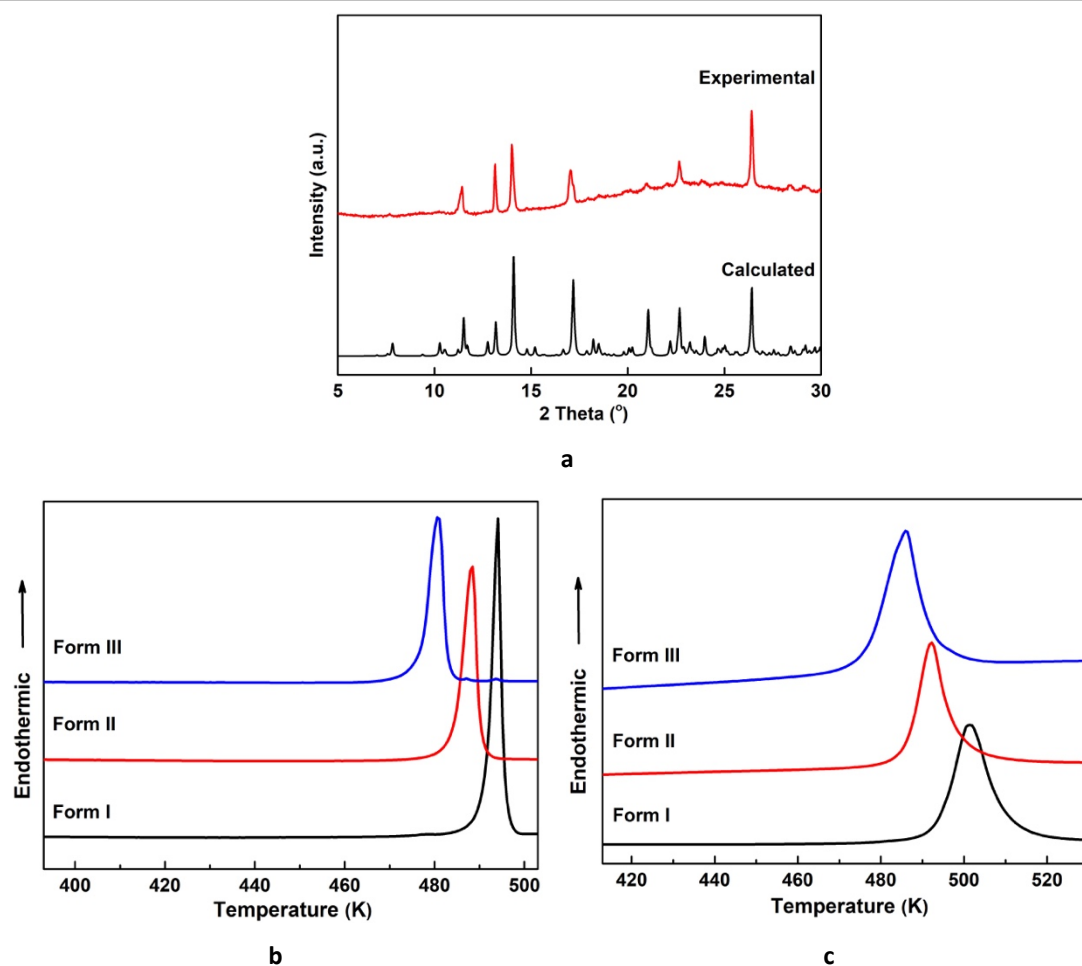
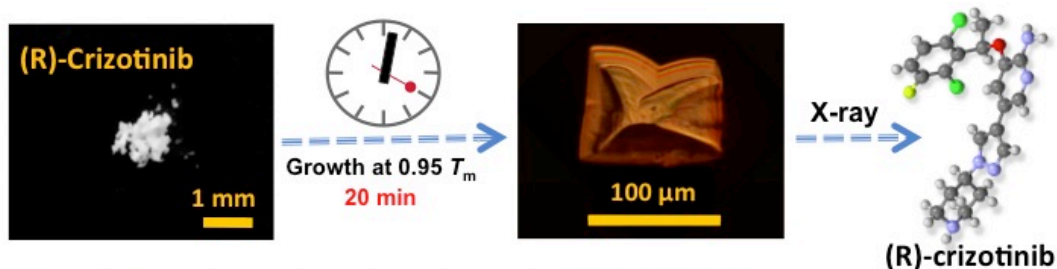


Figure S1. Experimental and calculated PXRD patterns of GSF Form III (a), and DSC curves of GSF polymorphs at the heating rate of 10 K/min (b) and 50 K/min (c).

3.3 Cultivation of single crystals of twenty clinical drugs using melt microdroplet method

(1) Crizotinib



Scheme S1. Single-crystal growth and absolute structure determination of crizotinib.

A small amount of commercial (R)-crizotinib powder was placed on a coverslip and partially melted around 478 K to yield a melt microdroplet containing a single seed crystal. This seed was harvested at 453 K in 20 min to yield a single crystal of $90 \mu\text{m} \times 110 \mu\text{m}$ (Scheme S1). X-ray data confirmed the R-configuration with the flack value of 0.017(11). The simulated PXRD pattern is consistent with the experimental data (Figure S2).

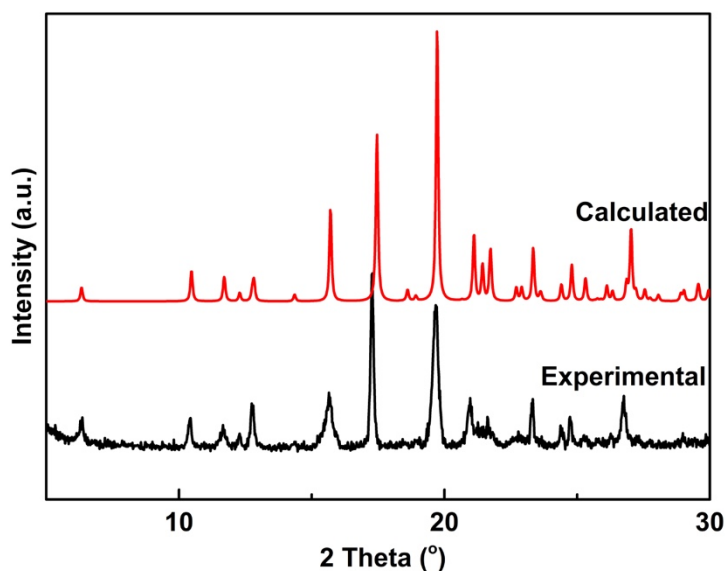


Figure S2. Experimental and calculated PXRD patterns of (R)-crizotinib.

Crystallographic data of (R)-crizotinib: C2 (5) space group, $a = 15.2412(4) \text{ \AA}$, $b = 10.1051(3) \text{ \AA}$, $c = 14.0138(4) \text{ \AA}$, $\beta = 100.491(3)^\circ$. $V = 2122.24 \text{ \AA}^3$, $Z' = 1$, $Z = 4$, R-factor = 6.17%.

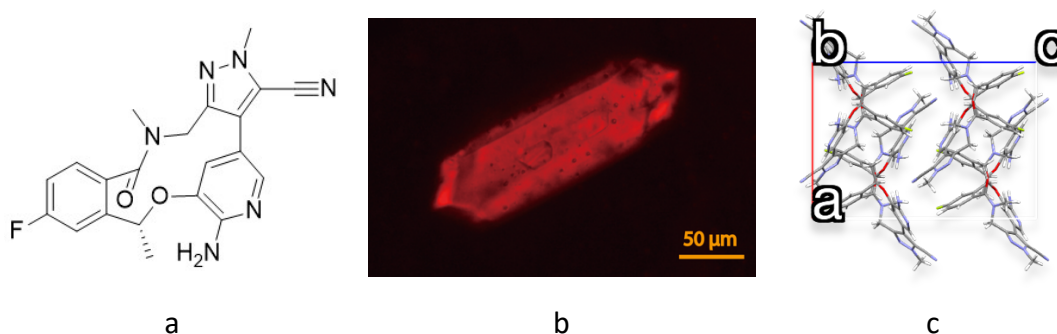
(2) Lorlatinib

Figure S3. Chemical structure (a), polarized optical microscopy (POM) image of single crystal (b) and crystal packing viewed along b-axis (c) of lorlatinib.

A small amount of commercial lorlatinib powder was partially melted to yield a melt microdroplet that contains only one seed. Because lorlatinib is a thermal sensitive drug and seriously degrades upon melting, this melt droplet was continuously cooled to let the seed grow to a sufficient size (170 μm × 50 μm) for X-ray diffraction (**Figure S3**). The simulated PXRD pattern is consistent with the experimental data (**Figure S4**).

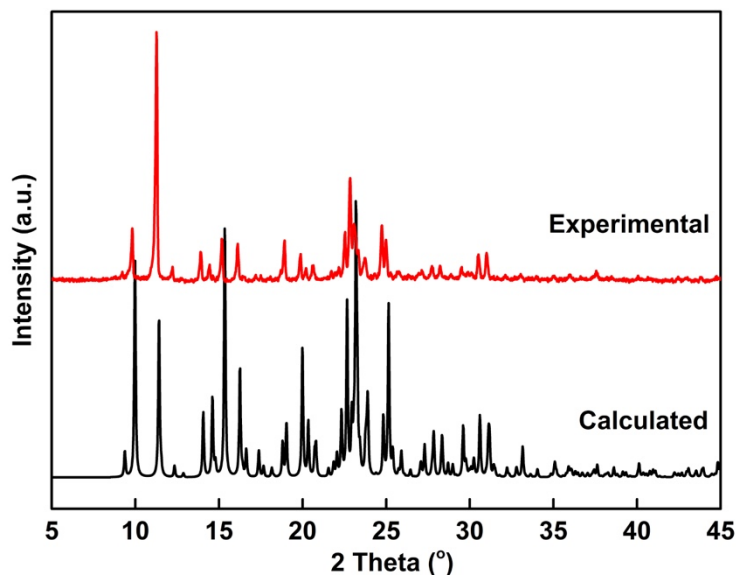


Figure S4. Experimental and calculated PXRD patterns of lorlatinib.

Crystallographic data of lorlatinib: Pbc_a (61) space group, $a = 13.16690(10)$ Å, $b = 15.49550(10)$ Å, $c = 18.85980(10)$ Å. $V = 3847.92$ Å³, $Z = 8$, $Z' = 1$, R-factor = 4.22%.

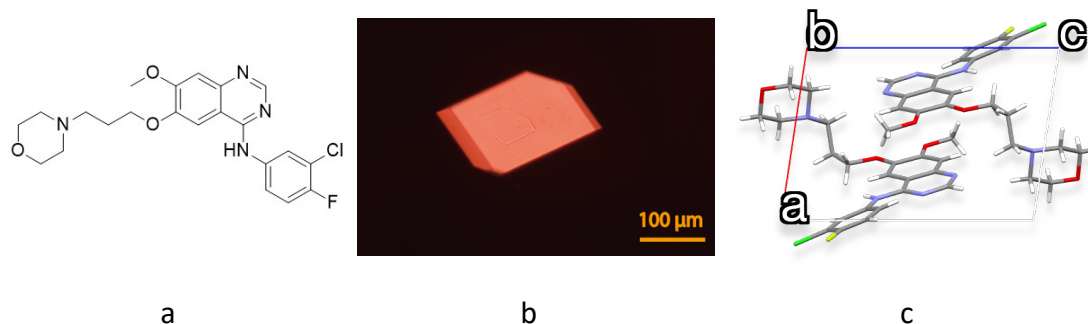
(3) Gefitinib

Figure S5. Chemical structure (a), POM image of single crystal (b) and crystal packing viewed along b-axis (c) of gefitinib.

A melt microdroplet that contains a single seed of gefitinib was obtained by partially melting a small amount of commercial powder at 468.5 K. This seed was then isothermally crystallized at 463 K in 10 min to yield a single crystal of 150 μm × 120 μm (**Figure S5**). The simulated PXRD pattern is consistent with the experimental data (**Figure S6**).

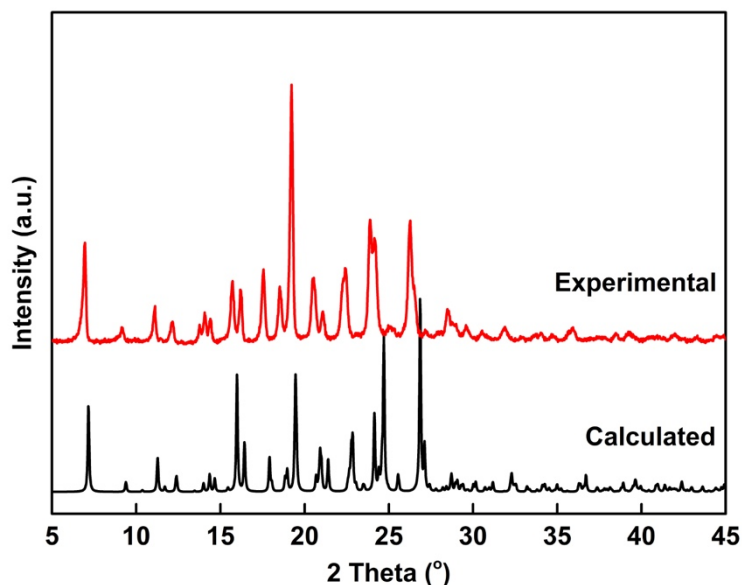


Figure S6. Experimental and calculated PXRD patterns of gefitinib.

Crystallographic data of gefitinib: $P\bar{1}$ (2) space group, $a = 8.81100(10)$ Å, $b = 9.6610(2)$ Å, $c = 12.4893(2)$ Å, $\alpha = 93.6600(10)^\circ$, $\beta = 97.5860(10)^\circ$, $\gamma = 101.8710(10)^\circ$. $V = 1026.74$ Å³, $Z = 2$, $Z' = 1$, R-factor = 3.4%, consistent with the reported structures of CCDC 259805, 819492 and 990393.

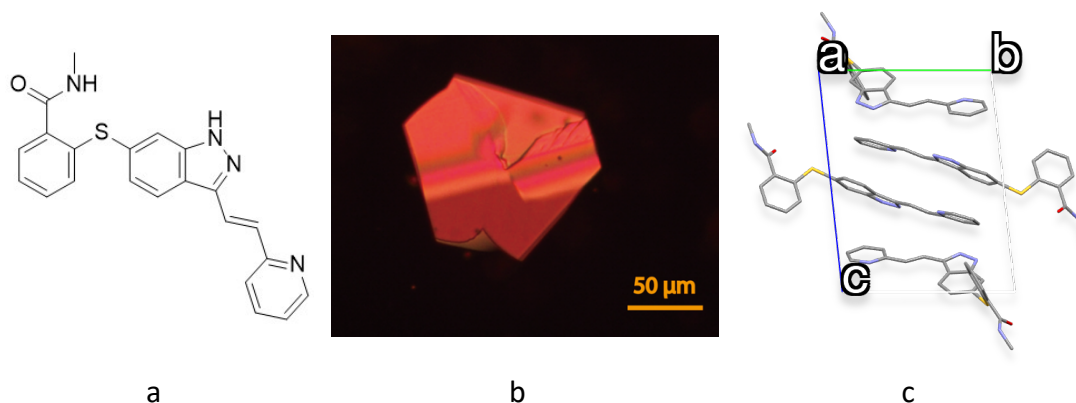
(4) Axitinib

Figure S7. Chemical structure (a), POM image of single crystal (b) and crystal packing viewed along a-axis (c) of axitinib.

A small amount of commercially available axitinib powder was partially melted around 495 K, yielding a single crystal seed in an isolated melt microdroplet. This seed crystal was grown at 483 K in 15 min to yield a single crystal of 100 $\mu\text{m} \times 90 \mu\text{m}$ (**Figure S7**). Crystallographic data indicated that this axitinib single crystal is triclinic with $P\bar{1}$ (2) space group ($a = 11.8120(2) \text{ \AA}$, $b = 12.3827(2) \text{ \AA}$, $c = 14.7603(2) \text{ \AA}$, $\alpha = 80.868(2)^\circ$, $\beta = 81.207(2)^\circ$, $\gamma = 65.701(2)^\circ$, $V = 1933.49 \text{ \AA}^3$, $Z = 4$, $Z' = 2$, R-factor = 5.49%). These data are consistent with the reported crystal structure of axitinib Form IV (CCDC 773994), while raw axitinib powder is Form I (refer to PXRD patterns in **Figure S8-a**). We heated the raw material by using DSC and observed that Form I melted around 483.8 K and then a new phase, Form IV, appeared with the melting point of 490.9 K^[2] (**Figure S8-b**). This result can explain why we used Form I powder as parent polycrystals, but obtained a single crystal of Form IV.

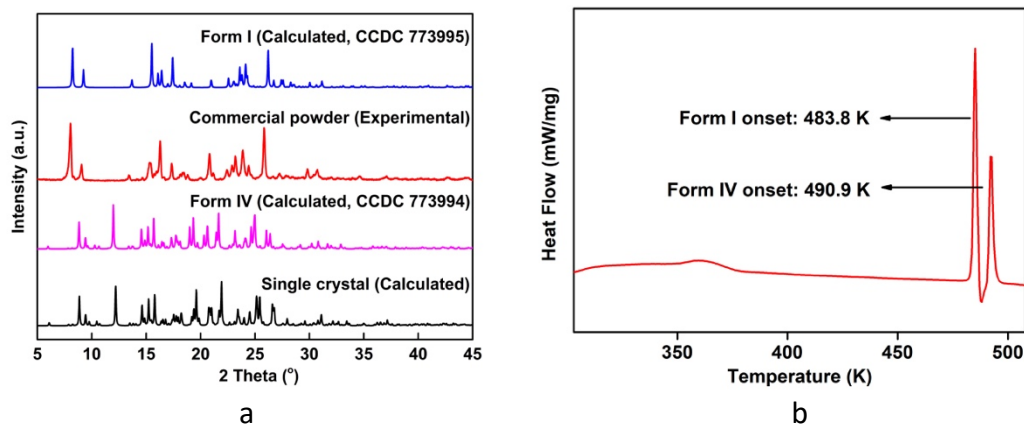


Figure S8. Experimental and calculated PXRD patterns of axitinib (a) and DSC curves of raw axitinib being heated at 10 K/min (b).

(5) Griseofulvin (Form I)

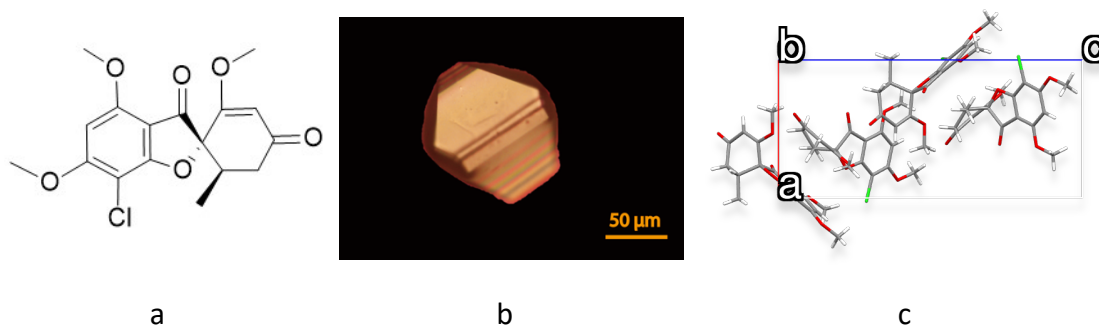


Figure S9. Chemical structure (a), POM image of single crystal (b) and crystal packing viewed along b-axis (c) of griseofulvin Form I.

A single seed of griseofulvin Form I in an isolated melt microdroplet was prepared by partial melting of a small amount of commercial polycrystalline powder at 494 K. This seed was grown at 488 K in 5min to yield a single crystal of $120\ \mu\text{m} \times 110\ \mu\text{m}$ (**Figure S9**). The simulated PXRD pattern based on single-crystal structure is consistent with the experimental data (**Figure S10**).

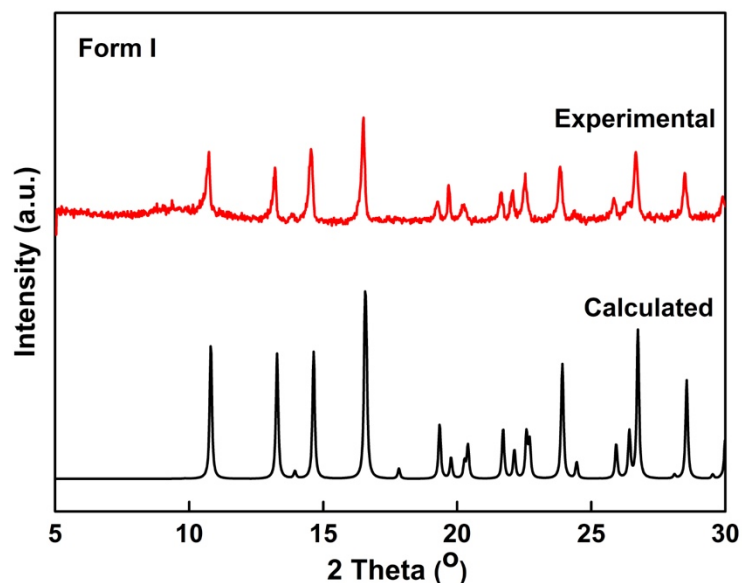


Figure S10. Experimental and calculated PXRD patterns of griseofulvin.

Crystallographic data of griseofulvin: $P4_1$ (76) space group, $a = 8.90270(10)\ \text{\AA}$, $b = 8.90270(10)\ \text{\AA}$, $c = 19.6158(2)\ \text{\AA}$. $V = 1554.71\ \text{\AA}^3$, $Z = 4$, $Z' = 1$, R-factor = 2.71%, consistent with the reported structure of CCDC 1170378 (Form I).

(6) Fluconazole

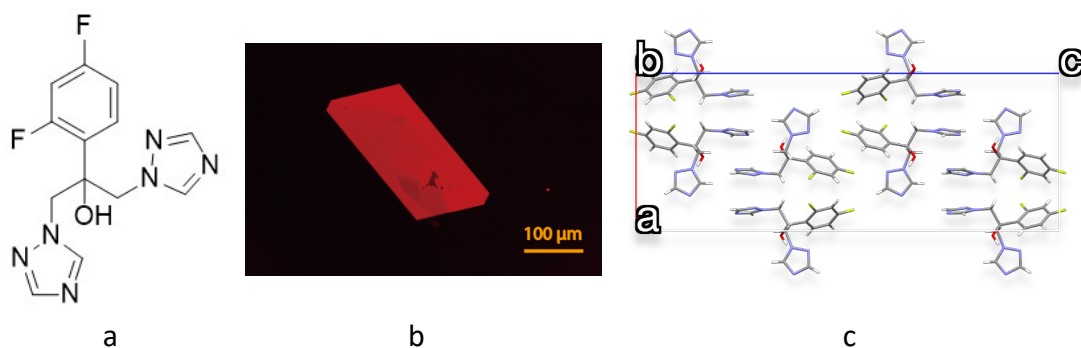


Figure S11. Chemical structure (a), POM image of single crystal (b) and crystal packing viewed along b-axis (c) of fluconazole.

To form a melt microdroplet that contains a single seed of fluconazole, a small amount of commercial fluconazole powder was partially melted around 414 K until all but a single seed remained. This seed was harvested at 409 K in 2 min, yielding a single crystal of $250\ \mu\text{m} \times 120\ \mu\text{m}$ (**Figure S11**). The simulated PXRD pattern highly matches the experimental data (**Figure S12**).

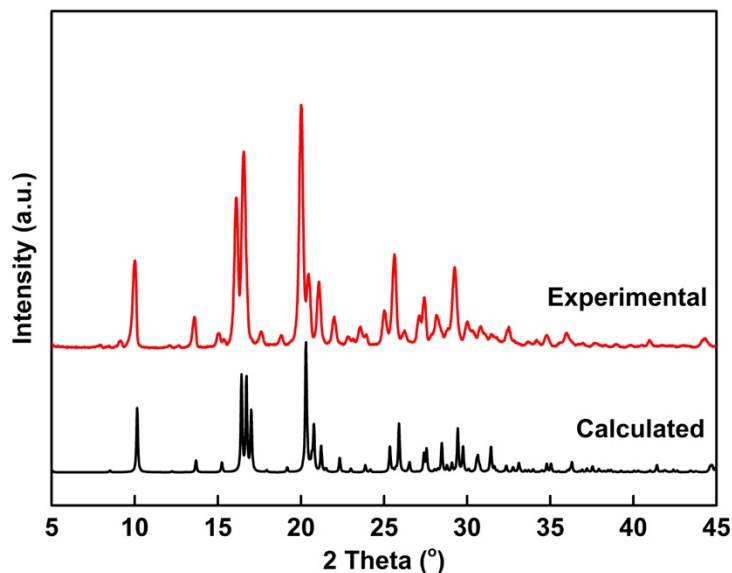


Figure S12. Experimental and calculated PXRD patterns of fluconazole.

Crystallographic data of Fluconazole: Pbca (61) space group, $a = 12.9345(2)\ \text{\AA}$, $b = 6.02210(10)\ \text{\AA}$, $c = 34.8527(8)\ \text{\AA}$. $V = 2714.78\ \text{\AA}^3$, $Z = 8$, $Z' = 1$, R-factor = 4.85%, consistent with the reported structures of CCDC 816586 and 1951672.

(7) Clotrimazole

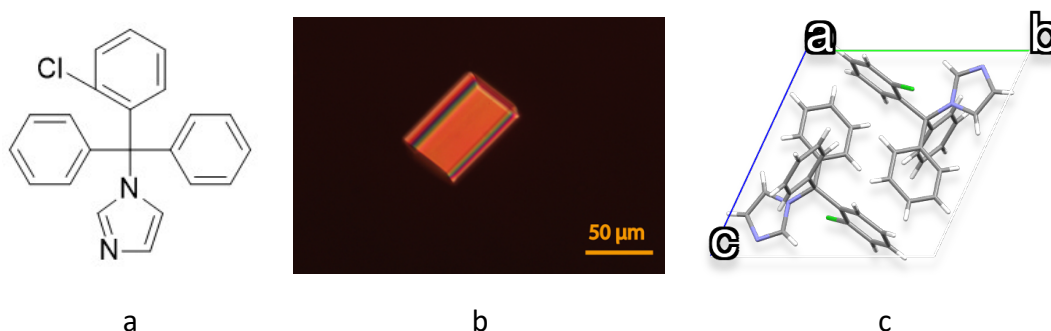


Figure S13. Chemical structure (a), POM image of single crystal (b) and crystal packing viewed along a-axis (c) of clotrimazole.

A small amount of commercial clotrimazole powder was partially melted around 421 K to yield a melt microdroplet that contains a single crystal seed. This seed was cultivated at 408 K in 70 min to yield a single crystal of 75 μm × 50 μm (**Figure S13**). The simulated PXRD pattern is consistent with the experimental data (**Figure S14**).

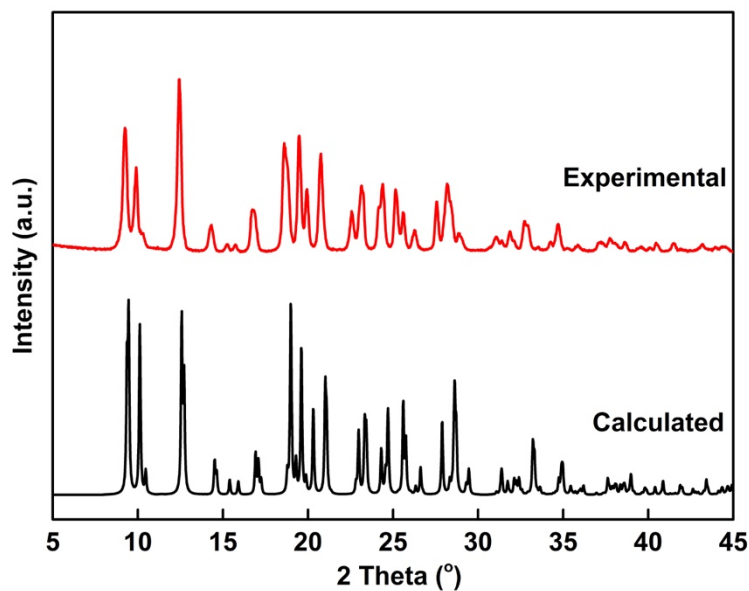


Figure S14. Experimental and calculated PXRD patterns of clotrimazole.

Crystallographic data of Clotrimazole: $P\bar{1}$ (2) space group, $a = 8.68460(10)$ Å, $b = 10.3809(2)$ Å, $c = 10.5107(2)$ Å, $\alpha = 113.566(2)^\circ$, $\beta = 97.7510(10)^\circ$, $\gamma = 96.7670(10)^\circ$. $V = 845.089$ Å³, $Z = 2$, $Z' = 1$, R-factor = 4.07%, consistent with the reported structure of CCDC 130537.

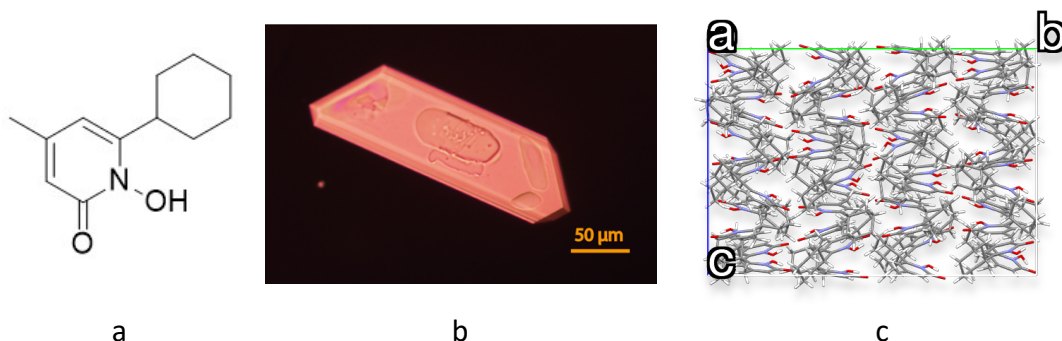
(8) Ciclopirox

Figure S15. Chemical structure (a), POM image of single crystal (b) and crystal packing viewed along a-axis (c) of ciclopirox.

To form a single crystal seed in an isolated microdroplet, a small amount of commercial ciclopirox powder was placed on a coverslip and partially melted around 416 K until all but a single seed remained. This seed rapidly grew to a single crystal of $375\ \mu\text{m} \times 125\ \mu\text{m}$ at 413 K in only 15 s (**Figure S15**). The simulated PXRD pattern fits the simulated PXRD pattern of CCDC 1406505 (**Figure S16**).

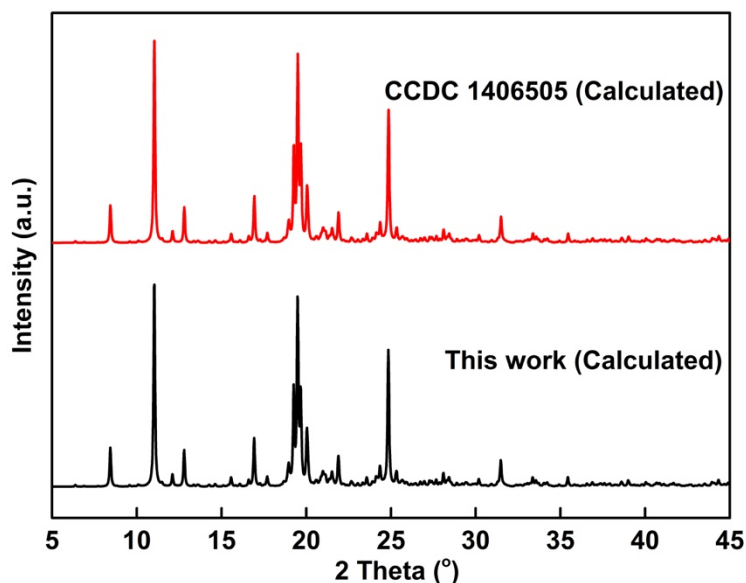


Figure S16. Experimental and calculated PXRD patterns of ciclopirox.

Crystallographic data of ciclopirox: $P2_1/c$ (14) space group, $a = 25.3104(4)\ \text{\AA}$, $b = 27.6509(4)\ \text{\AA}$, $c = 19.1485(2)\ \text{\AA}$, $\beta = 96.1260(10)^\circ$, $V = 13324.7\ \text{\AA}^3$, $Z = 48$, $Z' = 12$, R-factor = 7.72%, consistent with the reported structure of CCDC 1406505.

(9) Nifedipine

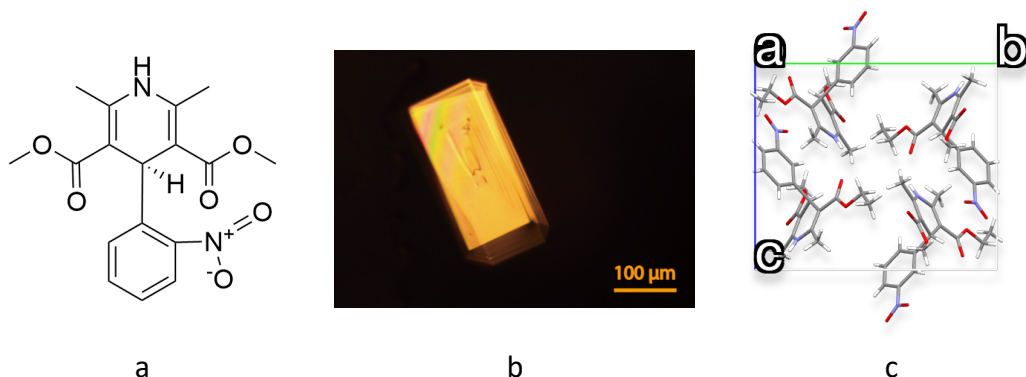


Figure S17. Chemical structure (a), POM image of single crystal (b) and crystal packing viewed along a-axis (c) of nifedipine.

A small quantity of commercially available powder of nifedipine was placed on a coverslip and partially melted around 448 K until all but a single crystal seed remained. This seed was allowed to grow in an isolated microdroplet at 443 K in 10 min, and thus yielded a single crystal of $275\ \mu\text{m} \times 175\ \mu\text{m}$ (**Figure S17**). The simulated PXRD pattern is consistent with the experimental data (**Figure S18**).

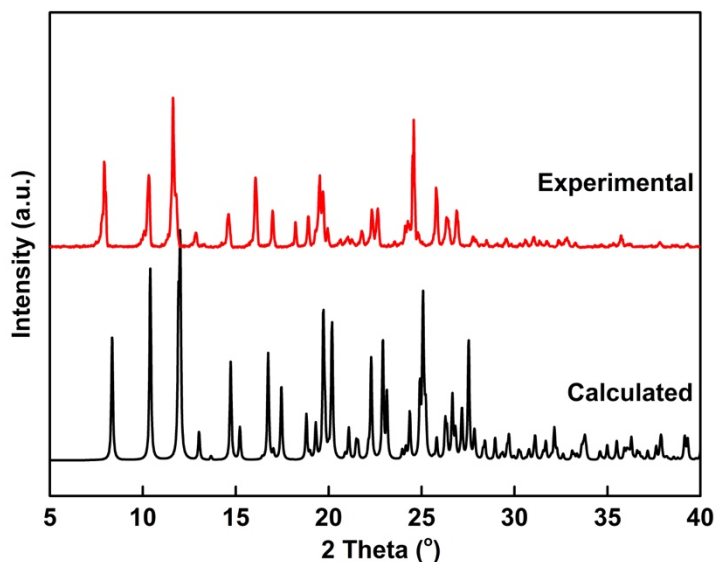


Figure 18. Experimental and calculated PXRD patterns of nifedipine.

Crystallographic data of nifedipine: $P2_1/c$ (14) space group, $a = 10.6219(4)\ \text{\AA}$, $b = 10.4085(4)\ \text{\AA}$, $c = 14.7800(5)\ \text{\AA}$, $\beta = 94.879(3)^\circ$, $V = 1628.13\ \text{\AA}^3$, $Z = 4$, $Z' = 1$, R-factor = 4.71%, consistent with the reported structure of CCDC 1110171.

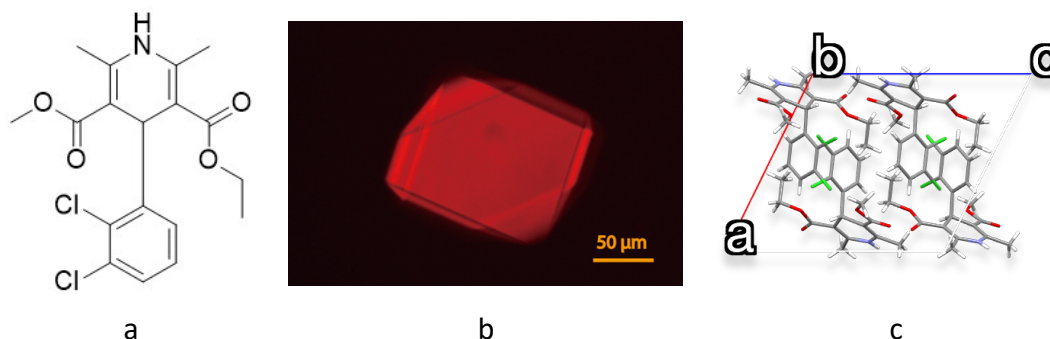
(10) Felodipine

Figure S19. Chemical structure (a), POM image of single crystal (b) and crystal packing viewed along b-axis (c) of felodipine.

By partial melting of felodipine polycrystals at 418 K, a melt microdroplet that contains a single crystal seed can be prepared. This seed can be allowed to grow at 408 K in 30 min to yield a single crystal with the size of 150 μm × 125 μm for X-ray diffraction (**Figure S19**). The simulated PXRD pattern highly matches the experimental data (**Figure S20**).

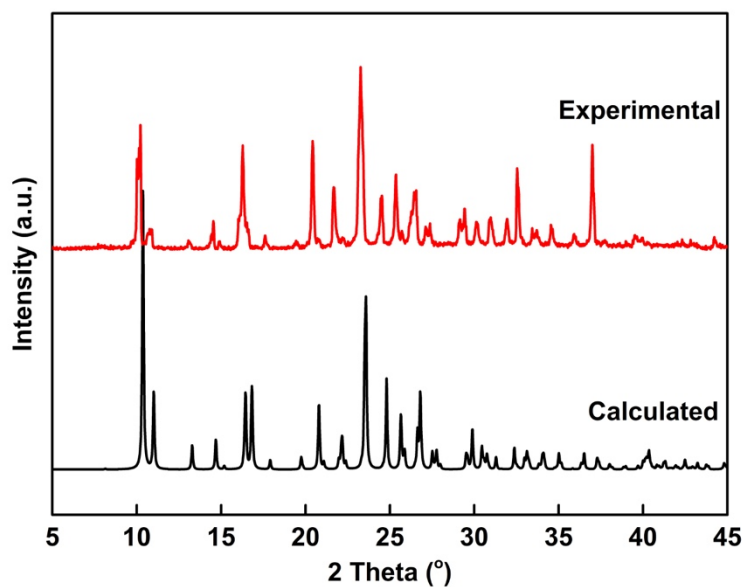


Figure S20. Experimental and calculated PXRD patterns of felodipine.

Crystallographic data of felodipine: $P2_1/c$ (14) space group, $a = 12.0936(2)$ Å, $b = 12.0624(2)$ Å, $c = 13.4258(2)$ Å, $\beta = 116.167(2)^\circ$, $V = 1757.8$ Å³, $Z = 4$, $Z' = 1$, R-factor = 7.82%, consistent with the reported structure of CCDC 1144175.

(11) Nimodipine

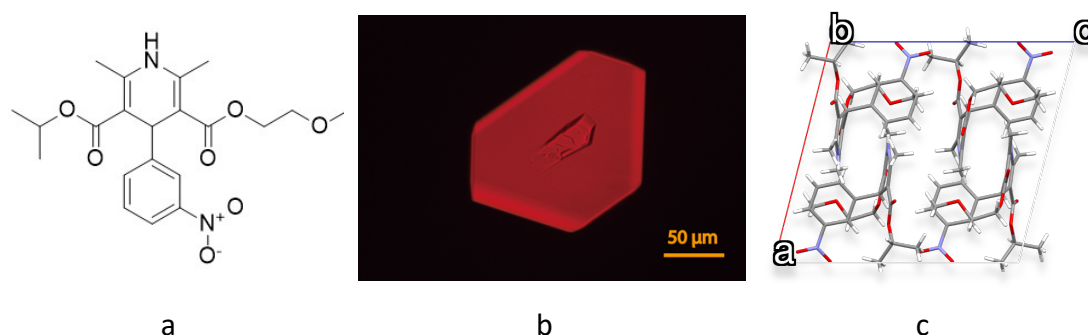


Figure S21. Chemical structure (a), POM image of single crystal (b) and crystal packing viewed along b-axis (c) of nimodipine.

Commercial powder of nimodipine was partially melted at 399 K until all but a single seed crystal remained. This seed was allowed to grow at 393 K in an *in-situ* formed microdroplet. After 20 min, a faceted single crystal yielded with the size of 175 μm \times 120 μm for X-ray diffraction (**Figure S21**). Crystallographic data indicated that this single crystal is monoclinic with $P2_1/c$ space group ($a = 13.76260(10)$ \AA , $b = 10.72760(10)$ \AA , $c = 14.78350(10)$ \AA , $\beta = 104.3000(10)^\circ$, $V = 2115$ \AA^3 , $Z = 4$, $Z' = 1$, R-factor = 4.47%). These data are consistent with the reported structure of Form I (CCDC 1280649), while the raw material is Form II (see **Figure S22**). Because nimodipine Form II was reported to transform to Form I during heating process,^[3] we speculated that commercial powder of nimodipine (Form II, metastable polymorph) converted to Form I (stable polymorph) during heating process, and thus both the seed and the resulting single crystal belong to Form I.

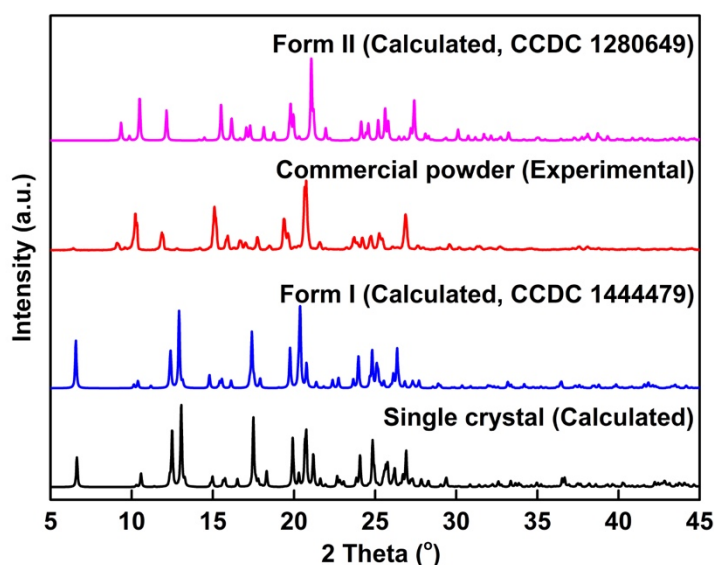


Figure S22. Experimental and calculated PXRD patterns of nimodipine.

(12) Nitrendipine

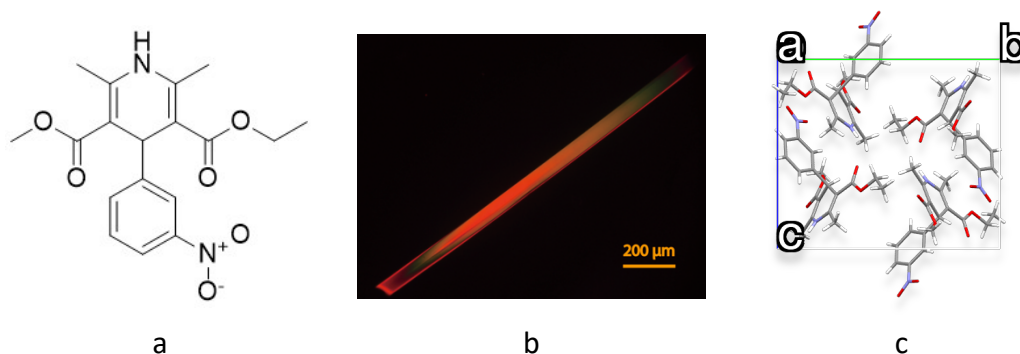


Figure S23. Chemical structure (a), POM image of single crystal (b) and crystal packing viewed along a-axis (c) of nitrendipine.

A small amount of commercial nitrendipine powder was partially melted around 434 K to yield a melt microdroplet that contains a single crystal seed. This seed was harvested at 421 K in 150 min and then yielded a single crystal of $60\text{ }\mu\text{m} \times 1400\text{ }\mu\text{m}$ (Figure S23). The simulated PXRD pattern highly matches with the experimental data (Figure S24).

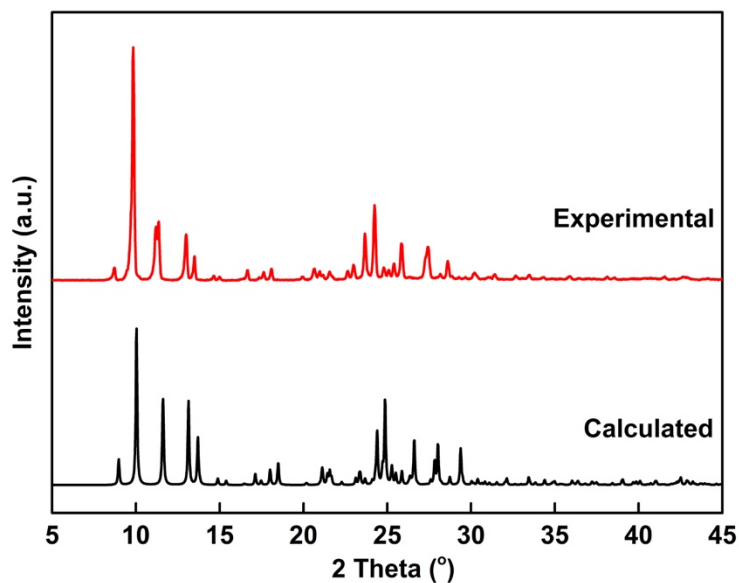


Figure S24. Experimental and calculated PXRD patterns of nitrendipine.

Crystallographic data of nitrendipine: $P2_1/c$ (14) space group, $a = 8.82590(10)\text{ }\text{\AA}$, $b = 15.2013(2)\text{ }\text{\AA}$, $c = 12.94740(10)\text{ }\text{\AA}$, $\beta = 93.7770(10)^{\circ}$, $V = 1733.32\text{ }\text{\AA}^3$, $Z = 4$, $Z' = 1$, R-factor = 7.66%, consistent with the reported structure of CCDC 1185426.

(13) Gliclazide

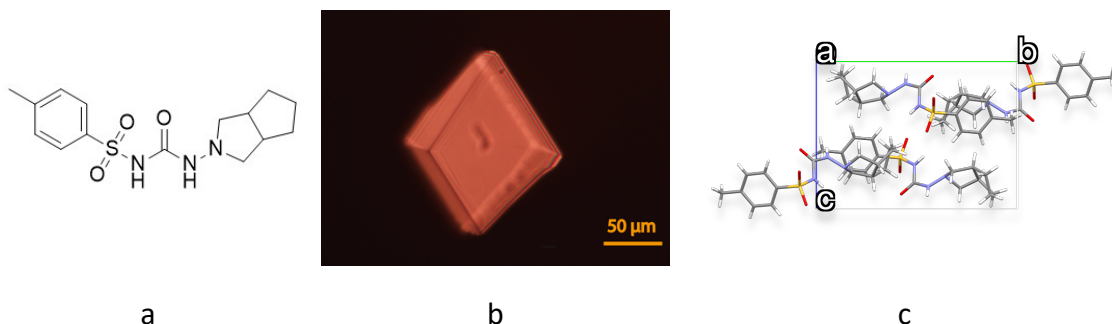


Figure S25. Chemical structure (a), POM image of single crystal (b) and crystal packing viewed along a-axis (c) of gliclazide.

A microdroplet that contains only one single seed crystal of gliclazide was prepared by partially melting commercial polycrystals at 453 K. Because gliclazide is a thermal sensitive drug and seriously degrades upon melting, this melt droplet was continuously cooled to let the seed grow to a sufficient size for X-ray diffraction (**Figure S25**). The simulated PXRD pattern is consistent with the experimental data (**Figure S26**).

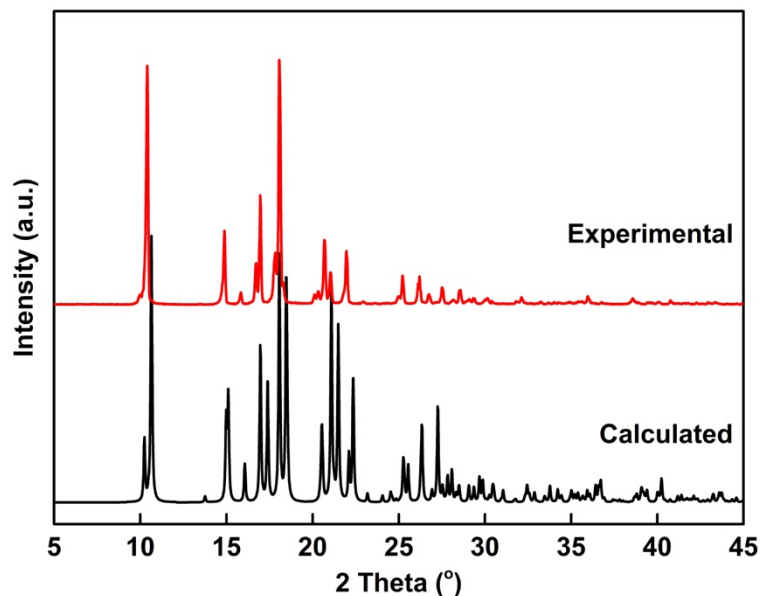


Figure S26. Experimental and calculated PXRD patterns of gliclazide.

Crystallographic data of gliclazide: $P2_1/n$ (14) space group, $a = 10.63520(10)$ Å, $b = 14.32960(10)$ Å, $c = 10.89950(10)$ Å, $\beta = 106.6230(10)^\circ$, $V = 1591.64$ Å³, $Z = 4$, $Z' = 1$, R-factor = 5.14 %, consistent with the reported structure of CCDC 130892.

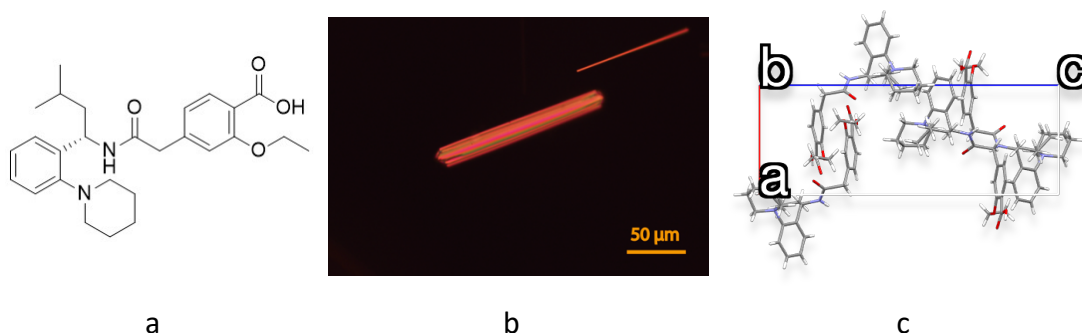
(14) Repaglinide

Figure S27. Chemical structure (a), POM image of single crystal (b) and crystal packing viewed along b-axis (c) of repaglinide.

A single crystal seed of repaglinide in an isolated microdroplet was obtained by partial melting of commercial raw material around 409 K. This seed was grown at 403 K in 10 min and then yielded a single crystal of 40 μm × 300 μm (**Figure S27**). X-ray diffraction data confirmed the R-configuration with the flack value of -0.01 (9). The simulated PXRD pattern is consistent with the experimental data (**Figure S28**).

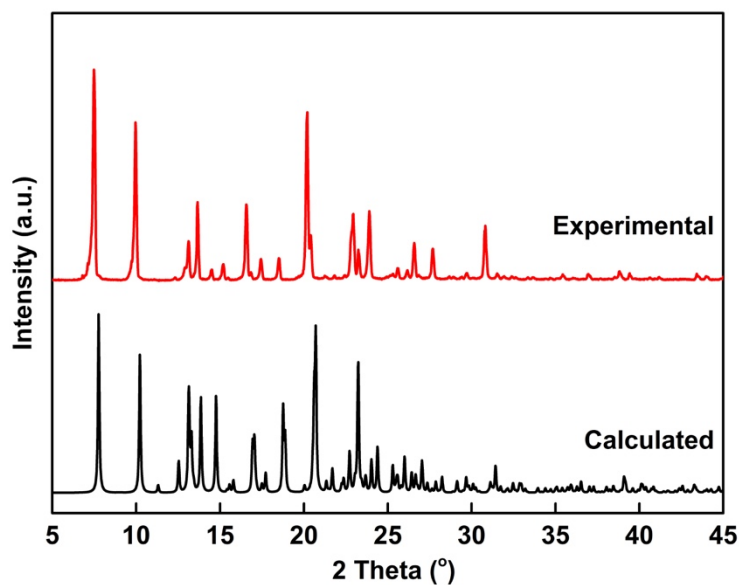


Figure S28. Experimental and calculated PXRD patterns of repaglinide.

Crystallographic data of repaglinide: $P2_12_12_1$ (19) space group, $a = 8.32210(10)$ Å, $b = 13.3053(2)$ Å, $c = 22.7527(3)$ Å. $V = 2519.36$ Å³, $Z = 4$, $Z' = 1$, R-factor = 3.7%, consistent with the reported structures of CCDC 117922 and 1858486.

(15) Metformin hydrochloride

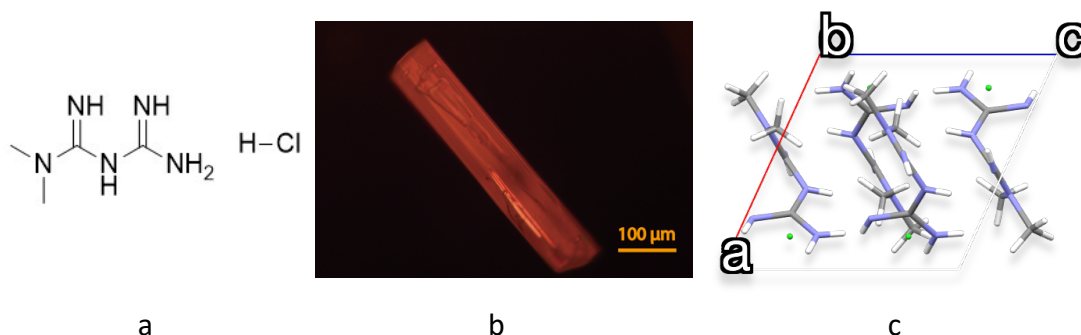


Figure S29. Chemical structure (a), POM image of single crystal (b) and crystal packing viewed along b-axis (c) of metformin hydrochloride.

A small amount of metformin hydrochloride powder was partially melted around 511 K to yield a microdroplet that contains only one crystal seed. This seed was cultivated at a relative low temperature, 433 K ($0.85 T_m$), to avoid the sublimation of metformin hydrochloride. After 30 min, a single crystal yielded with the size of $400 \mu\text{m} \times 70 \mu\text{m}$ for X-ray diffraction (**Figure S29**). The simulated PXRD pattern is in accordance with the experimental data (**Figure S30**).

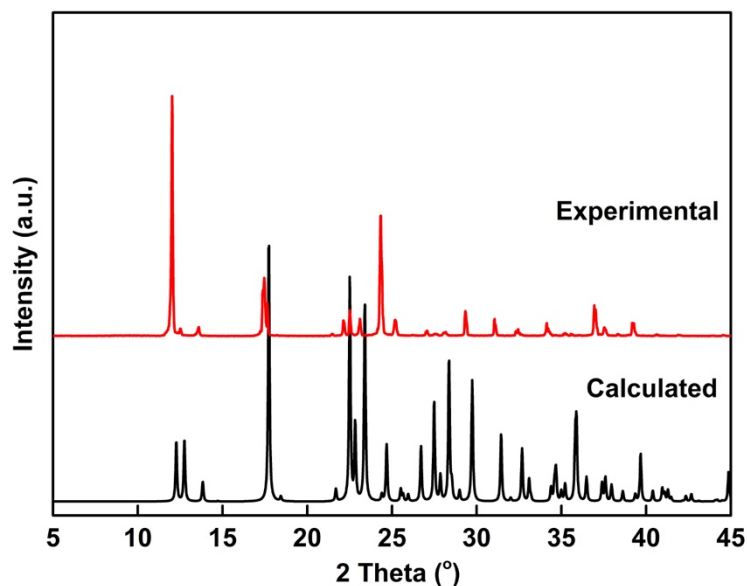


Figure S30. Experimental and calculated PXRD patterns of metformin hydrochloride.

Crystallographic data of metformin hydrochloride: $P 2_1/c$ (14) space group, $a = 7.9234(2) \text{ \AA}$, $b = 13.8743(2) \text{ \AA}$, $c = 7.9286(2) \text{ \AA}$, $\beta = 114.547(2)^\circ$, $V = 792.829 \text{ \AA}^3$, $Z = 4$, $Z' = 1$, $R\text{-factor} = 3.94\%$, consistent with the reported structures of CCDC 745429 and 1515490.

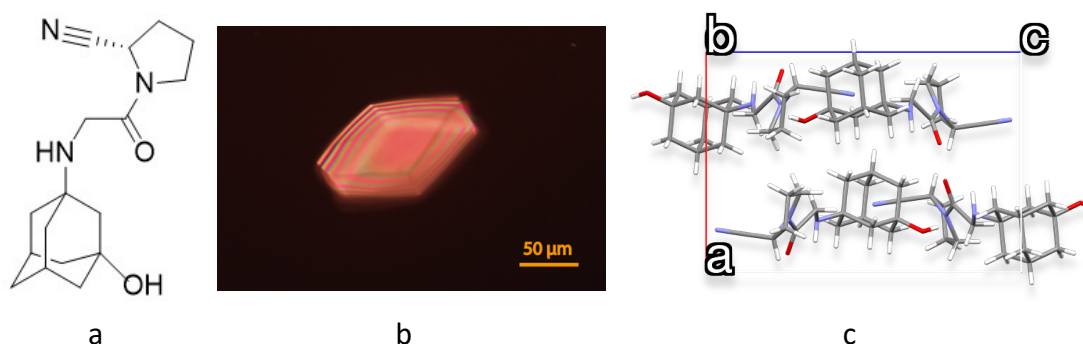
(16) Vildagliptin

Figure S31. Chemical structure (a), POM image of single crystal (b) and crystal packing viewed along b-axis (c) of vildagliptin.

A small amount of vildagliptin powder was partially melted around 428 K until all but a single seed remained. This seed was cultivated in an isolated microdroplet at 421 K for 15 min and then yielded a single crystal of 120 μm × 75 μm (**Figure S31**). X-ray diffraction data confirmed the R-configuration with the flack value of -0.06(11). The simulated PXRD pattern matches the experimental data (**Figure S32**).

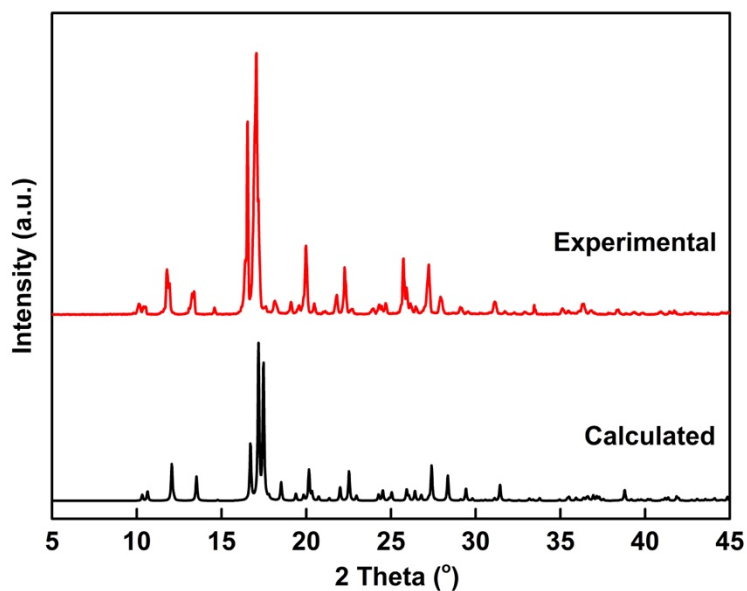


Figure S32. Experimental and calculated PXRD of vildagliptin.

Crystallographic data of vildagliptin: $P2_12_12_1$ (19) space group, $a = 10.14270(10)$ Å, $b = 10.60440(10)$ Å, $c = 14.51410(10)$ Å, $V = 1561.1$ Å³, $Z = 4$, $Z' = 1$, R-factor = 3.84%, consistent with the reported structure of CCDC 1107531.

(17) Paracetamol

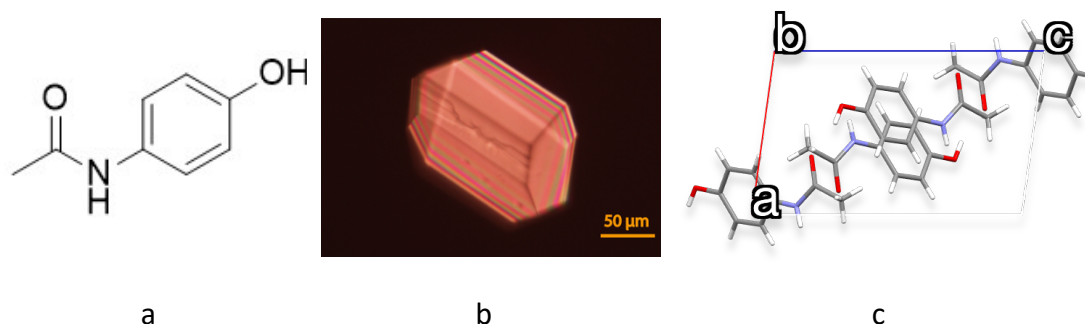


Figure S33. Chemical structure (a), POM image of single crystal (b) and crystal packing viewed along b-axis (c) of paracetamol.

To form a single crystal seed in an isolated microdroplet, a small amount of commercial paracetamol powder was placed on a coverslip and partially melted around 444 K. This seed was harvested at 440 K. After 5 min, it grew to a single crystal with the size of 140 μm × 100 μm for X-ray diffraction (**Figure S33**). The simulated PXRD pattern is in accordance with the experimental data (**Figure S34**).

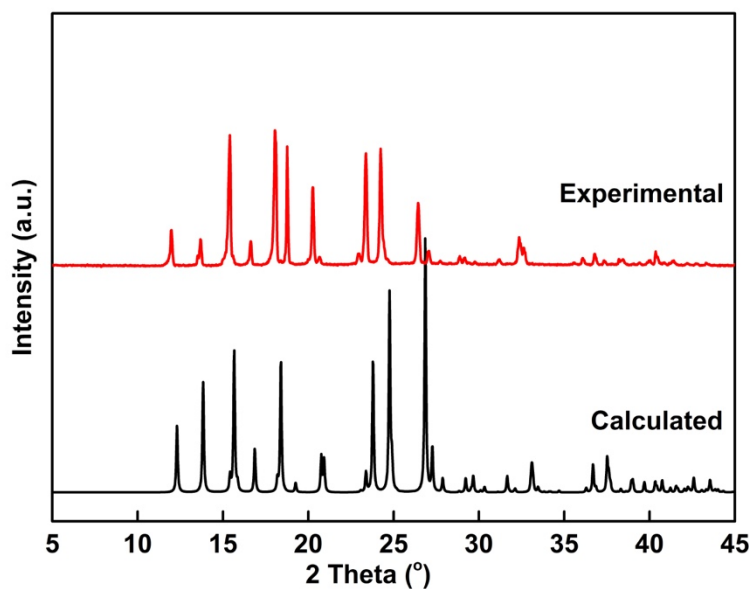


Figure S34. Experimental and calculated PXRD patterns of paracetamol.

Crystallographic data of paracetamol: $P2_1/n$ (14) space group, $a = 7.08950(10)$ Å, $b = 9.21120(10)$ Å, $c = 11.59660(10)$ Å, $\beta = 97.8900(10)^\circ$. $V = 750.122$ Å³, $Z = 4$, $Z' = 1$, R-factor = 4.24%, consistent with the reported structure of CCDC 1856579.

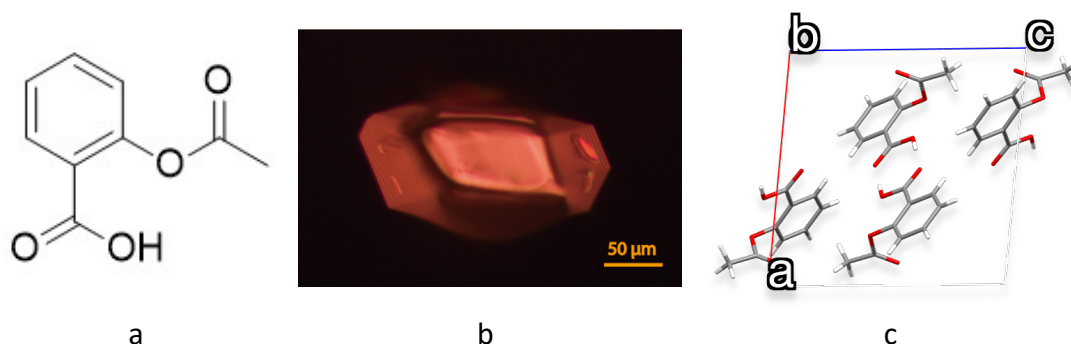
(18) Aspirin

Figure S35. Chemical structure (a), POM image of single crystal (b) and crystal packing viewed along b-axis (c) of aspirin.

A microdroplet containing only one crystal seed of aspirin was obtained by partial melting of commercial polycrystals at 415 K. This microdroplet was harvested at 408 K for 10 min to yield a single crystal of $180\ \mu\text{m} \times 80\ \mu\text{m}$ for X-ray diffraction (**Figure S35**). The simulated PXRD pattern highly matches the experimental data (**Figure S36**).

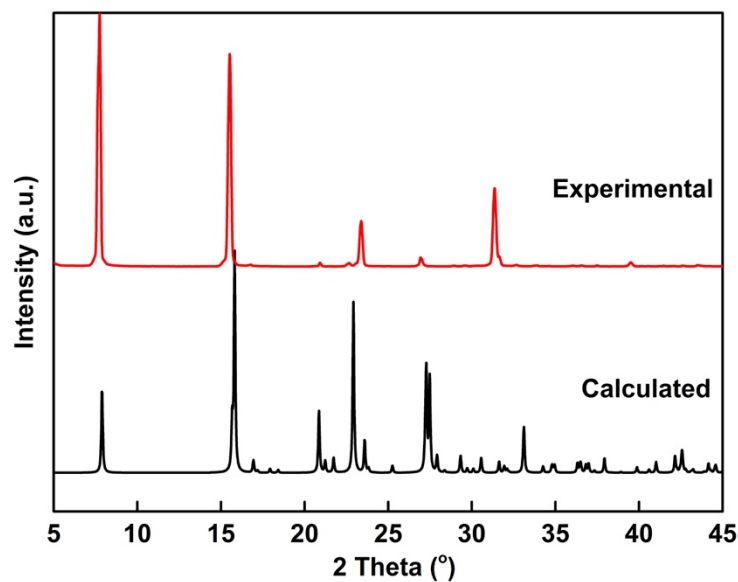


Figure S36. Experimental and calculated PXRD patterns of aspirin.

Crystallographic data of Aspirin: $P2_1/c$ (14) space group, $a = 11.2582(3)\ \text{\AA}$, $b = 6.54710(10)\ \text{\AA}$, $c = 11.2600(3)\ \text{\AA}$, $\beta = 95.949(2)^\circ$. $V = 825.489\ \text{\AA}^3$, $Z = 4$, $Z' = 1$, R-factor = 6.8%, consistent with the reported structures of CCDC 1101020, 1101021 and 195133.

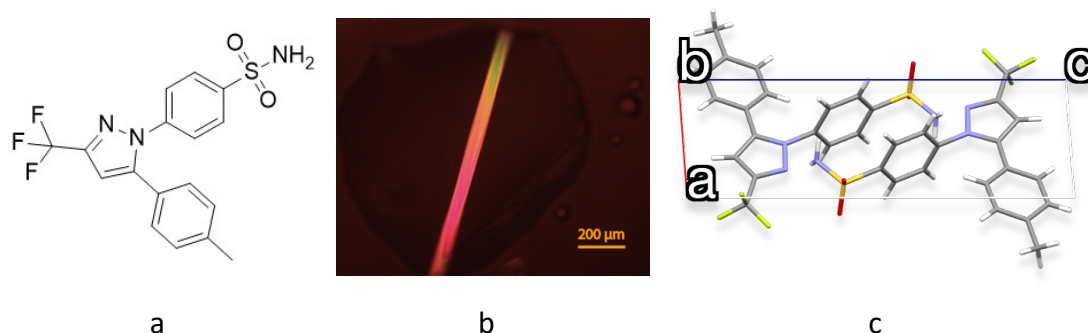
(19) Celecoxib

Figure S37. Chemical structure (a), POM image of single crystal (b) and crystal packing viewed along b-axis (c) of celecoxib.

Commercially available polycrystals of celecoxib was partially melted around 436 K and yielded a melt microdroplet containing a single-crystal seed. This seed was grown at 433 K for 20 min and then yielded a single crystal of 850 μm × 50 μm (**Figure S37**). The simulated PXRD pattern is consistent with the experimental data (**Figure S38**).

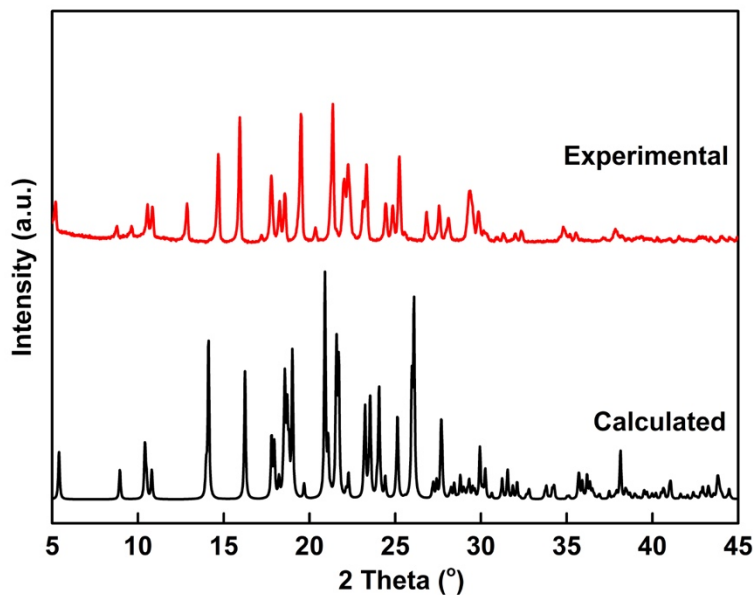


Figure S38. Experimental and calculated PXRD patterns of celecoxib.

Crystallographic data of celecoxib: $P\bar{1}$ (2) space group, $a = 5.06400(10)$ Å, $b = 10.01390(10)$ Å, $c = 16.40730(10)$ Å, $\alpha = 89.8820(10)^\circ$, $\beta = 85.8650(10)^\circ$, $\gamma = 80.5380(10)^\circ$, $V = 818.524$ Å³, $Z = 2$, $Z' = 1$, R-factor = 3.51%, consistent with the reported structure of CCDC 1875184.

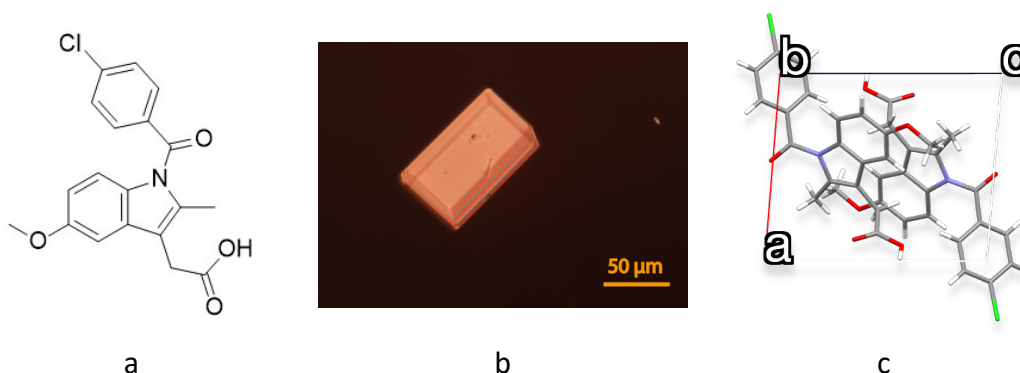
(20) Indomethacin

Figure S39. Chemical structure (a), POM image of single crystal (b) and crystal packing viewed along b-axis (c) of indomethacin.

By partially melting raw indomethacin powder at 436 K, a single-crystal seed in a microdroplet was obtained and then was cultivated at 423 K. After 30 min, this seed grew to a single crystal with the size of 80 μm \times 50 μm for X-ray diffraction (**Figure S39**). The simulated PXRD pattern highly matches the experimental data (**Figure S40**).

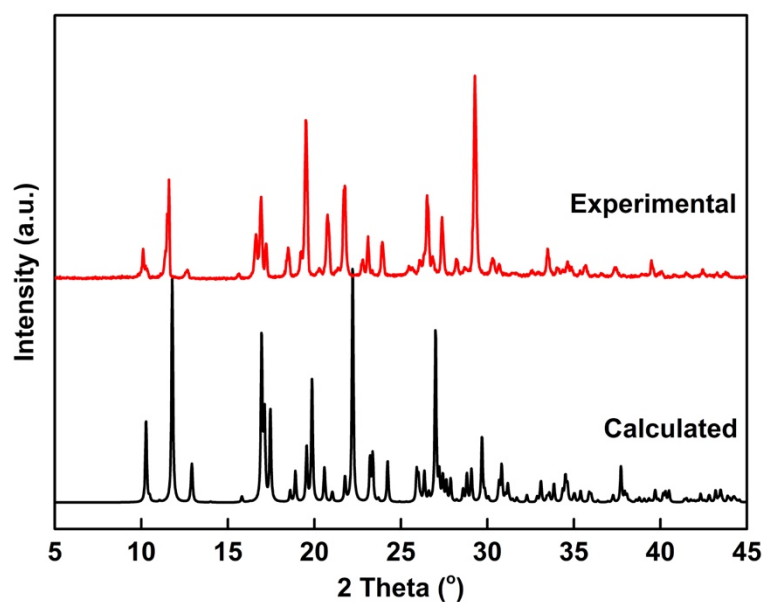


Figure S40. Experimental and calculated PXRD patterns of indomethacin.

Crystallographic data of indomethacin: $P\bar{1}$ (2) space group, $a = 9.21730(10)$ \AA , $b = 9.6060(2)$ \AA , $c = 10.8436(2)$ \AA , $\alpha = 69.959(2)^\circ$, $\beta = 87.1970(10)^\circ$, $\gamma = 69.501(2)^\circ$, $V = 842.093$ \AA^3 , $Z = 2$, $Z' = 1$, R-factor = 3.3%, consistent with the reported structure of CCDC 217467.

SUPPORTING INFORMATION

Table S1. Summary of cultivation conditions for twenty-two single crystals

No.	Compound	T_m (K)	T_{growth} (K)	t_{growth} (min)	T_{growth}/T_m	Size (μm)	Test temperature (K)	CCDC number
1	Crizotinib	478	453	20	0.94770	110 × 90	100	1945591
2	Lorlatinib	NA	NA	Cooling	NA	170 × 50	298	1987322
3	Gefitinib	468.5	463	10	0.98826	150 × 120	100	1987320
4	Axitinib	495	483	15	0.97576	100 × 90	100	1987321
5	Griseofulvin (Form I)	494	488	5	0.98785	120 × 110	100	1893055 ^[4]
6	Fluconazole	414	409	2	0.98792	250 × 120	100	1987331
7	Clotrimazole	421	408	70	0.96912	75 × 50	100	1987332
8	Ciclopirox	416	413	0.25	0.99522	375 × 125	100	1987333
9	Nifedipine	448	443	10	0.98884	275 × 175	100	1918294
10	Felodipine	418	408	30	0.97608	150 × 125	100	1987340
11	Nimodipine	399	393	20	0.98496	175 × 120	100	1987341
12	Nitrendipine	434	421	150	0.97005	1400 × 60	100	1987339
13	Gliclazide	453	NA	Cooling	NA	100 × 100	100	1987345
14	Repaglinide	409	403	10	0.98533	300 × 40	100	1987346
15	Metformin HCl	511	433	30	0.84736	400 × 70	100	1987347
16	Vildagliptin	428	421	15	0.98364	120 × 75	100	1987348
17	Paracetamol	444	440	5	0.99099	140 × 100	100	1987511
18	Aspirin	415	408	10	0.98313	180 × 80	100	1987510
19	celecoxib	436	433	20	0.99312	850 × 50	100	1987512
20	Indomethacin	436	423	30	0.97018	80 × 50	100	1987513
21	Griseofulvin (Form II)	488	478	15	0.97951	130 × 130	100	1918290
22	Griseofulvin (Form III)	478	473	25	0.98954	490 × 320	100	1893057 ^[5]

NA: not available.

References

- [1] D. Zhou, G. G. Z. Zhang, D. Law, D. J. W. Grant, E. A. Schmitt, *Molecular Pharmaceutics* 2008, **5**, 927-936.
- [2] A. M. Campeta, B. P. Chekal, Y. A. Abramov, P. A. Meenan, M. J. Henson, B. Shi, R. A. Singer, K. R. Horspool, *Journal of Pharmaceutical Sciences* 2010, **99**, 3874-3886.
- [3] N. L. Calvo, N. M. Balzaretta, M. Antonio, T. S. Kaufman, R. M. Maggio, *Journal of Pharmaceutical and Biomedical Analysis* 2018, **158**, 461-470.
- [4] M. Lu, CCDC 1893055: Experimental Crystal Structure Determination, 2019, DOI: 10.5517/ccdc.csd.cc21jw9s.
- [5] M. Lu, CCDC 1893057: Experimental Crystal Structure Determination, 2019, DOI: 10.5517/ccdc.csd.cc21jwcv.